# Reconstruction of Dawsonite by Alumina Carbonation in $(NH_4)_2CO_3$: Requisites and Mechanism

Georgiana Stoica,[†] Johan C. Groen,[‡] Sònia Abelló,[†] Ripudaman Manchanda,[†] and Javier Pérez-Ramírez*[,†,§]

*Institute of Chemical Research of Catalonia (ICIQ), Avinguda Països Catalans 16, 43007 Tarragona, Spain, DelftChemTech, Delft University of Technology, Julianalaan 136, 2628 BL Delft, The Netherlands, and Catalan Institution for Research and Advanced Studies (ICREA), Passeig Lluís Companys 23, 08010 Barcelona, Spain*

*Received February 4, 2008. Revised Manuscript Received April 4, 2008*

The products derived from thermal decomposition of $NH_4$, K, and Na dawsonites have structural memory; that is, the original mineral structure in ammonium form ($NH_4AlCO_3(OH)_2$) is recovered upon treatment of the oxide in aqueous $(NH_4)_2CO_3$ solution under mild conditions at pH ∼ 10. The memory effect holds in aluminas doped with transition metals such as chromium or iron. In contrast, treatment of calcined dawsonites in $K_2CO_3$ and $Na_2CO_3$ solutions leads to bayerite. The mechanism and kinetics of the reconstruction process were investigated by experiments in a parallel-reactor system varying treatment time, temperature, molar $(NH_4)_2CO_3/Al_2O_3$ ratio, $(NH_4)_2CO_3$ concentration, solvent, and dawsonite composition. The samples at different stages of the treatment in ammonium carbonate were characterized by X-ray diffraction, infrared spectroscopy, transmission and scanning electron microscopies, nitrogen adsorption, mercury intrusion porosimetry, and thermogravimetry. The reconstruction of the dawsonite structure from alumina follows a dissolution−precipitation mechanism and is accomplished in 10−30 min depending on the temperature. The transformation goes through an intermediate carbonate-containing aluminum hydroxide compound of amorphous nature followed by progressive dawsonite crystallization upon ammonium incorporation. In contrast with other families of materials having structural memory such as hydrotalcites, the original and reconstructed dawsonites present marked morphological and porosity differences. Upon reconstruction, nanoparticles in the as-made and calcined materials gradually transformed by way of complex intermediate morphologies into acicular nanoneedles with newly developed microporosity. The facile carbonation of alumina-related compounds in ammonium carbonate is potentially applicable for $CO_2$ mineralization.

## Introduction

Considerable effort is being deployed to develop smart materials and structures for creating hitherto novel products and for performance enhancement of existing products in a broad range of applications. Smart materials have the ability to respond in a controlled manner to external stimuli, such as mechanical deformation, stress, pressure, temperature, chemicals, incident radiation, electric and magnetic fields, electric charges, and so forth.[1] Materials responses to these types of stimuli include the rearrangement of atomic and molecular structures, the creation and motion of crystallographic defects, chemical reactions, absorption and emission of photons, generation of charge and voltage, and other effects. Well-known examples of smart materials are piezoelectric sensors,[2] shape-memory metal alloys,[3] shape-memory polymers,[4] magnetic-memory metal alloys,[5] halochromic and chromogenic systems,[6] and compounds with structural memory.[7,8]

In the context of the latter category, hydrotalcite-like compounds can be considered as prototypic materials. This family of anionic clays consists of brucite-like layers that transform into high-surface-area well-dispersed mixed oxides on calcination.[9,10] The oxide is able to recover the original layered structure in contact with humid gas, water, and aqueous salt solutions.[7,9,11–17] The memory property of

* Corresponding author. Fax: +34 977 920 224. E-mail: jperez@iciq.es.
[†] Institute of Chemical Research of Catalonia (ICIQ).
[‡] Delft University of Technology.
[§] Catalan Institution for Research and Advanced Studies (ICREA).

(1) Wilson, A. R. In *Kirk-Othmer Encyclopedia of Chemical Technology*; Seidel, A., Ed.; John Wiley & Sons, Inc.: New York, 2006; Vol. 22, pp 705−722.
(2) Lang, S. B.; Muensit, S. *Appl. Phys. A: Mater. Sci. Process.* **2006**, *85*, 125.
(3) Hornbogen, E. *Adv. Eng. Mater.* **2006**, *8*, 101.
(4) Ratna, D.; Karger-Kocsis, J. *J. Mater. Sci.* **2008**, *43*, 254.
(5) Kainuma, R.; Imano, Y.; Ito, W.; Sutou, Y.; Morito, H.; Okamoto, S.; Kitakami, O.; Oikawa, K.; Fujita, A.; Kanomata, T.; Ishida, K. *Nature* **2006**, *439*, 957.
(6) Lampert, C. M. *Mater. Today* **2004**, *7*, 28.
(7) Braterman, P. S.; Xu, Z. P.; Yarberry, F. In *Handbook of Layered Materials*; Auerbach, S. M.; Carrado, K. A.; Dutta, P. K., Eds.; Taylor & Francis: New York, 2004; pp 313−372.
(8) Stoica, G.; Pérez-Ramírez, J. *Chem. Mater.* **2007**, *19*, 4783.
(9) Cavani, F.; Trifiro, F.; Vaccari, A. *Catal. Today* **1991**, *11*, 173.
(10) Reichle, W. T. *J. Catal.* **1985**, *94*, 547.
(11) Kooli, F.; Depège, C.; Ennaqadi, A.; Roy, A. D.; Besse, J. P. *Clays Clay Miner.* **1997**, *45*, 92.
(12) Marchi, A. J.; Apesteguía, C. R. *Appl. Clay Sci.* **1998**, *13*, 35.
(13) Millange, F.; Walton, R. I.; O'Hare, D. *J. Mater. Chem.* **2000**, *10*, 1713.
(14) van Bokhoven, J. A.; Roelofs, J. C. A. A.; de Jong, K. P.; Koningsberger, D. C. *Chem. Eur. J.* **2001**, *7*, 1258.

10.1021/cm800359t CCC: $40.75 
Published on Web 05/30/2008

hydrotalcites has multiple applications: removal of anions in contaminated water,[18,19] development of drug delivery systems,[20,21] and insertion of new functionalities and active catalytic sites.[22,23] The retrotopotactic transformation in hydrotalcites is accepted to occur via a dissolution−precipitation mechanism,[24,25] by which the regeneration takes place through crystallization from solution. The poorly crystalline nature of the mixed oxide derived by calcination of hydrotalcites is thought to be key in the attainment of the memory effect.[17] As anticipated for a reversible transformation, the platelet-like morphology and type of mesoporosity in the original and reconstructed hydrotalcites are essentially maintained.[16,26]

We have recently extended the unique structural memory property of oxides derived from hydrotalcites to dawsonite-type compounds.[8] Natural dawsonite is a mineral with formula $NaAlCO_3(OH)_2$ exhibiting various crystal habits including prisms, aciculae, fibers, spheres, rosettes, and random aggregates.[27] It exhibits an orthorhombic-dipyramidal structure, consisting of an assemblage of edge-sharing distorted $AlO_2(OH)_4$ and $NaO_4(OH)_2$ octahedra and $CO_3^{2-}$ groups.[28,29] One oxygen of the carbonate is hydrogen-bonded to two hydroxyl groups, strengthening the three-dimensional framework.[28] Besides $NaAlCO_3(OH)_2$, a variety of compositions with dawsonite-type structure have been synthesized by changing the nature of sodium or aluminum cations in the structure.[30–32] Potassium and ammonium dawsonites are the most studied analogues of the mineral and are composed of the same $AlO_2(OH)_4$ chains of octahedra as the dawsonite mineral. The structure of K dawsonite is visualized in Figure 1. The $NH_4$-analogue, that is, $NH_4AlCO_3(OH)_2$, is often denoted as ammonium aluminum carbonate hydroxide or by the acronym AACH. Our earlier work[8] demonstrated that amorphous and low-skeleton density aluminas obtained by decomposition of AACH at 523 and 723 K reform the original dawsonite structure upon treatment in 1 M $(NH_4)_2CO_3$ solution at 323 K and ambient pressure for 24 h according to

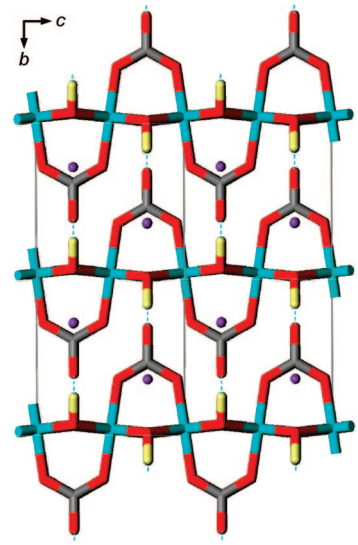


**Figure 1.** Structure of potassium dawsonite ($KAlCO_3(OH_2)$) in the (100) direction. Cell parameters and atomic coordinates taken from Fernández-Carrasco et al.[47] K, purple spheres; Al, blue sticks; C, grey sticks; O, red sticks; and H, yellow sticks. Dashed lines represent hydrogen bonds.

$$Al_2O_3 + 2NH_4^+ + 2HCO_3^- + H_2O \rightarrow 2NH_4AlCO_3(OH)_2 \quad (1)$$

The retrotopotactic transformation of dawsonite did not solely imply the recovery of the original structure but also originated changes in composition, morphology, and porosity with respect to the parent material.[8] That study attained dawsonite reconstruction from AACH-derived $Al_2O_3$ by $(NH_4)_2CO_3$ treatment in a single set of conditions with respect to temperature, time, and composition of the starting dawsonite. Consequently, a detailed mechanistic and kinetic picture of the reconstruction process was not provided. This understanding is needed to exploit the memory property of this family of materials. For example, the ability of tailoring the physicochemical characteristics (shape, size, porosity) by reconstruction may have an impact on the properties of dawsonite in reported applications as antiacid, polymer stabilizer, fertilizer additive, flame retardant, adsorbent for industrial flue gases, and catalyst precursor.[33–38] Besides, the carbonation of alumina leading to dawsonite (eq 1) is linked to $CO_2$ mineralization, a topic of great environmental relevance for alleviating global warming. Several authors reported that dawsonite is a product of $CO_2$ trapping by aluminosilicate minerals, such as feldspars, at high pressure.[27,39] Accordingly, investigating the interaction of alumina with carbonate-containing solutions is interesting to preliminarily

(15) Abelló, S.; Medina, F.; Tichit, D.; Pérez-Ramírez, J.; Groen, J. C.; Sueiras, J. E.; Salagre, P.; Cesteros, Y. *Chem. Eur. J.* **2005**, *11*, 728.
(16) Pérez-Ramírez, J.; Abelló, S.; van der Pers, N. M. *Chem. Eur. J.* **2007**, *13*, 870.
(17) Pérez-Ramírez, J.; Abelló, S.; van der Pers, N. M. *J. Phys. Chem. C* **2007**, *111*, 3642.
(18) Palomares, A. E.; Prato, J. G.; Rey, F.; Corma, A. *J. Catal.* **2004**, *221*, 62.
(19) Shiraga, M.; Kawabata, T.; Li, D.; Shishido, T.; Komaguchi, K.; Sano, T.; Takehira, K. *Appl. Clay Sci.* **2006**, *33*, 247.
(20) Nakayama, H.; Wada, N.; Tsuhako, M. *Int. J. Pharm.* **2004**, *269*, 469.
(21) Williams, G. R.; O'Hare, D. *J. Mater. Chem.* **2006**, *16*, 3065.
(22) Rives, V.; Ulibarri, M. A. *Coord. Chem. Rev.* **1999**, *181*, 61.
(23) Tichit, D.; Coq, B. *CATTECH* **2003**, *7*, 206.
(24) Rajamathi, M.; Nataraja, G. D.; Ananthamurthy, S.; Kamath, P. V. *J. Mater. Chem.* **2000**, *10*, 2754.
(25) Stanimirova, T. S.; Kirov, G.; Dinolova, E. *J. Mater. Sci. Lett.* **2001**, *20*, 453.
(26) Prinetto, F.; Ghiotti, G.; Graffin, P.; Tichit, D. *Microporous Mesoporous Mater.* **2000**, *39*, 229.
(27) Bénézeth, P.; Palmer, D. A.; Anovitz, L. M.; Horita, J. *Geochim. Cosmochim. Acta* **2007**, *71*, 4438.
(28) Frueh, A. J.; Golightly, J. P. *Can. Mineral.* **1967**, *9*, 51.
(29) Corazza, E.; Sabelli, C.; Vannucci, S. *Neues Jahrb. Mineral. Monatsh.* **1977**, *9*, 381.
(30) Serna, C. J.; Garcia-Ramos, J. V.; Peña, M. J. *Spectrochim. Acta* **1985**, *41A*, 697.
(31) Ali, A. A.; Hasan, M. A.; Zaki, M. I. *Chem. Mater.* **2005**, *17*, 6797.
(32) Yalfani, M. S.; Santiago, M.; Pérez-Ramírez, J. *J. Mater. Chem.* **2007**, *17*, 1222.
(33) Serna, C. J.; White, J. L.; Hem, S. L. *J. Pharm. Sci.* **1978**, *67*, 324.
(34) Bonsignore, P. V. *Plast. Eng.* **1976**, *32*, 41.
(35) Gillman, G.; Noble, A. *Environmental Quality Management* **2005**, *15*, 59.
(36) Altman, R. L.; Mayer, L. A.; Ling, A. C. U.S. Patent 4,406,797, 1983.
(37) Doyle, J. B.; Pirsh, E. D. A.; Downs, W. EP0268353, 1988.
(38) Santiago, M.; Yalfani, M. S.; Pérez-Ramírez, J. *J. Mater. Chem.* **2006**, *16*, 2886.
(39) Hellevang, H.; Aagaard, P.; Oelkers, E. O.; Kvamme, B. *Environ. Sci. Technol.* **2005**, *39*, 8281.

assess the potential of Al-containing compounds in sequestration of carbon dioxide.

This paper reports the mechanism and kinetics of dawsonite recrystallization from amorphous alumina by carbonation in aqueous $(NH_4)_2CO_3$ solution. Reconstruction is specific to ammonium carbonate, since treatment in other carbonate salts such as $K_2CO_3$ and $Na_2CO_3$ leads to bayerite. The influence of time, temperature, reconstruction media (salt and solvent), molar $(NH_4)_2CO_3/Al_2O_3$ ratio, $(NH_4)_2CO_3$ concentration, and chemical composition and precipitation conditions of the original dawsonite on the reconstruction process have been investigated using a parallel reactor system. Structural, morphological, and porosity changes along the course of the treatment have been systematically studied by a number of characterization techniques, and key factors conferring the unique memory feature to this family of materials are discussed.

## Experimental Section

**Materials and Treatments.** $NH_4-Al$, $K-Al$, and $Na-Al$ dawsonites were synthesized by coprecipitation at constant pH using the in-line dispersion−precipitation (ILDP) method.[40] Briefly, aqueous solutions of $Al(NO_3)_3 \cdot 9H_2O$ (1.1 M) and the precipitating agent ($(NH_4)_2CO_3$, $K_2CO_3$, or $Na_2CO_3$, 2 M) were continuously fed to the miniaturized precipitation chamber (volume of ca. 6 mL), which was stirred at 13 500 rpm. The synthesis was carried out at pH 8 or 10 (by adjusting the flow of the basic solution) with an average residence time of 18 s. The resulting slurry was aged at 333 K for 3 h, followed by filtration, washing, and drying at 333 K for 12 h. Metal-substituted aluminum dawsonites with a molar Fe:Al or Cr:Al ratio of 1:11 were prepared in the same way by incorporating $Cr(NO_3)_3 \cdot 9H_2O$ and $Fe(NO_3)_3 \cdot 9H_2O$ (0.1 M) in the 1.1 M $Al^{3+}$ solution. The as-synthesized samples were calcined in static air at 723 K during 2 h using a heating rate of 5 K $min^{-1}$.

Reconstruction experiments were conducted in a fully automated Multimax liquid-phase parallel chemical synthesizer from Mettler Toledo, consisting of 16 parallel-batch glass reactors (17 mm i.d., total volume 50 $cm^3$) in four independent blocks and enabling high-throughput experimentation.[41,42] The treatment consisted in dispersing the oxide powder in a solution under magnetic stirring (350 rpm). The influence of various parameters such as time (0−30 min), temperature (298−343 K), media ($(NH_4)_2CO_3$, $K_2CO_3$, $Na_2CO_3$), concentration of the carbonate salt (0.01−2 M), molar $(NH_4)_2CO_3/Al_2O_3$ ratio (2−25), solvent (water, methanol), and dawsonite composition (A−Al where A = $NH_4$, K, Na, and $NH_4$-($B_x$-$Al_{1+x}$) where B = Fe, Cr and $x = 0$ or 0.1) on the reconstruction process was investigated. The treated samples were filtered, thoroughly washed with deionized water until the pH of the filtrate was 7, and dried at 333 K for 12 h. All chemicals used were purchased from Panreac and Sigma-Aldrich and had purities > 98%. Along the manuscript, the as-synthesized, calcined, and reconstructed samples are generally identified by the codes AS, C, and R, respectively. The number in the code of the reconstructed samples (e.g., R-30) refers to the treatment time in minutes. If not explicitly mentioned, the AS sample refers to $NH_4-Al$ dawsonite.

**Techniques.** Powder X-ray diffraction patterns were acquired using a Bruker AXS D8 Advance diffractometer equipped with a Cu tube, a Ge(111) incident beam monochromator ($\lambda = 0.1541$ nm), and a Vantec-1 PSD. Data were recorded in the $2\theta$ range of 10−70° with an angular step size of 0.016° and a counting time of 6 s per step. Fourier transform infrared spectroscopy was carried out in a Bruker Optics Tensor 27 spectrometer equipped with a Golden Gate Diamond ATR unit. Spectra were collected at room temperature in the range 650−4000 $cm^{-1}$ by coaddition of 32 scans at a nominal resolution of 4 $cm^{-1}$, taking the spectrum of the empty cell at ambient conditions as the background. Transmission electron microscopy was carried out in a JEOL JEM-1011 microscope operated at 80 kV and equipped with a SIS Megaview III CCD camera. A few droplets of the sample suspended in ethanol were placed on a carbon-coated copper grid followed by evaporation at ambient conditions. Environmental scanning electron microscopy (ESEM) was carried out in a FEI Quanta 600 FEG microscope operated at 30 kV. Nitrogen adsorption−desorption isotherms at 77 K were measured on a Quantachrome Autosorb-6B analyzer. Before analysis, the samples were degassed in vacuum at 373 K for 16 h. The BET method[43] was applied to calculate the total surface area, and the *t*-plot method[44] was used to discriminate between micro- and mesoporosity. The BJH model[45] applied to the adsorption branch of the isotherm provided information on the mesopore size distribution. Mercury porosimetry was measured on Pascal 140 and 440 porosimeters (Thermo Electron), which operate in the pressure range of 0.001−400 MPa. Prior to the intrusion−extrusion experiment, the sample was degassed ($10^{-1}$ Pa) at 373 K for 16 h. Thermogravimetric analysis (TGA) was carried out in a Mettler Toledo TGA/SDTA851e microbalance. The solid (3 mg) was placed in 70 $\mu$L α-alumina crucibles without dilution. Analyses were performed in dry air flow of 50 $cm^3$ STP $min^{-1}$, ramping the temperature from 298 to 1173 K at 5 K $min^{-1}$.

## Results and Discussion

**Reconstruction Kinetics.** Our previous work[8] reported the reconstruction of the dawsonite structure from amorphous alumina derived from calcination of AACH (ammonium aluminum carbonate hydroxide) by treatment under the following conditions: 1 M $(NH_4)_2CO_3$ aqueous solution, $(NH_4)_2CO_3/Al_2O_3$ ratio of 25, 323 K, and 24 h. As stressed in the Introduction, a wider examination of conditions is needed to gain in-depth mechanistic and kinetic understanding of the reconstruction process. This includes temperature, time, concentration, molar ratio of reactants, reconstruction media, and chemical composition of the starting dawsonite.

X-ray diffraction makes it possible to follow the evolution in time of amorphous alumina to crystalline dawsonite upon treatment at the above conditions (Figure 2). The solid remains amorphous in the first stages of the treatment and the characteristic (110) reflection of the dawsonite phase at $2\theta = 15°$ becomes discernible after 8 min in the ammonium carbonate aqueous solution at 323 K. No intermediate phase of crystalline nature was detected in this transition. The X-ray diffraction pattern of ammonium dawsonite ($NH_4Al(CO_3)(OH)_2$, JCPDS 42-250) was fully developed after approximately 15 min. Longer treatment times led to dawsonite crystallization as the diffraction lines progressively get sharper and more intense. The experiment illustrated in

(40) Abelló, S.; Pérez-Ramírez, J. *J. Adv. Mater.* **2006**, *18*, 2436.
(41) Abelló, S.; Dhir, S.; Colet, G.; Pérez-Ramírez, J. *Appl. Catal., A* **2007**, *325*, 121.
(42) Groen, J. C.; Moulijn, J. A.; Pérez-Ramírez, J. *Ind. Eng. Chem. Res.* **2007**, *46*, 4193.
(43) Brunauer, S.; Emmett, P. H.; Teller, E. *J. Am. Chem. Soc.* **1938**, *60*, 309.
(44) Lippens, B. C.; de Boer, J. H. *J. Catal.* **1965**, *4*, 319.
(45) Barret, E. P.; Joyner, L. G.; Hallenda, P. H. *J. Am. Chem. Soc.* **1951**, *73*, 373.

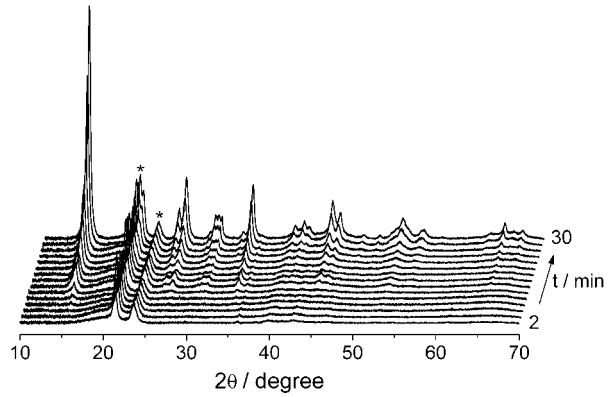


**Figure 2.** XRD patterns during treatment of AACH-derived alumina in 1 M $(NH_4)_2CO_3$ aqueous solution at 323 K. The reflections marked with asterisks are due to the sample holder.

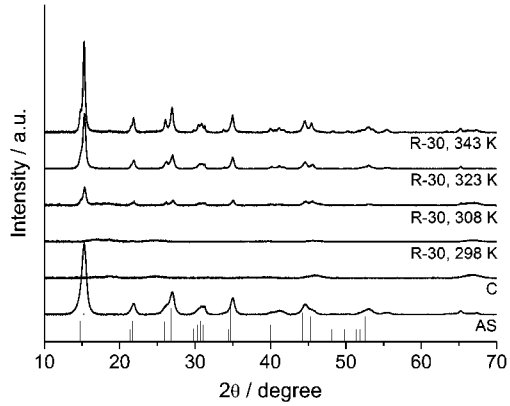


**Figure 3.** XRD patterns of the as-synthesized, calcined, and reconstructed samples at different temperatures for 30 min. The starting dawsonite was in the ammonium form, and the reconstruction of the oxide was conducted in 1 M $(NH_4)_2CO_3$ aqueous solution. Vertical lines belong to $NH_4Al(CO_3)(OH)_2$ (JCPDS 42-250).

Figure 2 was conducted at different temperatures in the range of 298−343 K maintaining other conditions expressed above. For the sake of conciseness, Figure 3 shows the XRD patterns of the solids after treatment at different temperatures for 30 min. The diffractograms of the as-synthesized dawsonite (AS) and calcined product at 723 K (C) are also shown for comparison. Sample C exhibits very broad reflections at $2\theta = 45°$ and 67°, indicating the presence of tiny crystallites of $\gamma$-$Al_2O_3$ (JCPDS 29-63) in the subnanometer range. The pattern of the sample upon 30 min treatment at 298 K in 1 M $(NH_4)_2CO_3$ did not show any sign of reconstruction. dawsonite reconstruction was accelerated upon increasing temperature from 308 to 343 K, since the diffraction lines of the mineral-like phase become sharper and more intense at the same treatment time. Consequently, the time at which the first reflection of dawsonite appeared in a similar experiment to that shown in Figure 2 was shorter on increasing the treatment temperature: 20 min at 308 K, 8 min at 323 K, and only 4 min at 343 K. In other words, the carbonation of alumina to dawsonite in $(NH_4)_2CO_3$ at 343 K is 2 and 5 times faster than at 323 and 308 K, respectively. Besides, comparison of R-30 treated at 323 and 343 K with AS in Figure 3 indicates sharper reflections in the reconstructed samples, indicative of the occurrence of larger crystals than in the as-synthesized dawsonite. The average crystallite size, estimated by the Scherrer formula in the (110) reflection, was approximately 4−6 times larger in the R-30 samples (25 nm at 323 K and 35 nm at 343 K) than in the AS sample (6 nm). This further confirms that the structural retrotransformation of AACH-derived alumina to dawsonite is accompanied by a marked crystal growth, which we have referred to as dawsonite *reforming*.[8]

The influence of the concentration of the ammonium carbonate solution and the molar ratio of ammonium carbonate to alumina were also investigated. The experiments reported earlier[8] and in Figures 2 and 3 applied 1 M $(NH_4)_2CO_3$ aqueous solution (pH 10) and an excess of ammonium carbonate ($(NH_4)_2CO_3/Al_2O_3 = 25$) compared to the stoichiometric ratio of 2 according to eq 1. As anticipated, the structural memory of dawsonite is also manifested when the ammonium carbonate to alumina ratio was 10 and 2. The reconstruction proceeds in a similar time scale for all ratios at 323 K with respect to the appearance of the first dawsonite reflection, and the crystallite sizes after 30 min treatment did not vary significantly. The pH of the ammonium carbonate solution plays an important role on the reconstruction process. No sign of dawsonite formation or any other transformation was observed after 30 min at 323 K when the $(NH_4)_2CO_3$concentration was 0.2 M (pH 8.8). It can be inferred that the pH of this solution does not ensure the minimum concentration of ions required to convert alumina into dawsonite. Increasing the concentration to 0.5 M and up to 2 M leads to pH in the relatively narrow range of 9.5−10.5, where dawsonite formation within the practiced treatment time of 30 min occurred. The next section further elaborates on the influence of pH on the product of alumina treatment in solutions of different carbonate salts and concentrations.

**Influence of dawsonite Composition and Treatment Media.** Reconstruction treatments have so far been conducted over $NH_4$−Al dawsonite. To determine how general the memory property is, the dependence of the process on the chemical composition of the starting material has been studied. The main results of the treatments are summarized in Table 1. First of all, we have investigated whether dawsonite can be recovered if transition metals are structurally incorporated during the synthesis. It is known that this type of material can accommodate different cations in $Al^{3+}$ positions.[31] Single-phased iron and chromium-substituted $NH_4$ dawsonites, denoted as $Fe_{0.1}$-$Al_{1.1}$ and $Cr_{0.1}$-$Al_{1.1}$, were successfully synthesized (Figure 4). As expected, calcination of the precipitates at 723 K for 2 h led to an amorphous oxidic phase; that is, no reflections specific to crystalline $Fe_2O_3$, $Cr_2O_3$, or $Al_2O_3$ were identified. Treatment of the oxide in 1 M $(NH_4)_2CO_3$ aqueous solution at 323 K for 30 min induced the recovery of the dawsonite phase, largely resembling the transformation experienced by the sample without transition metals.

Similarly to $NH_4$−Al dawsonite, Na−Al and K−Al dawsonites were synthesized by precipitation at pH 8, using $Na_2CO_3$ and $K_2CO_3$ as precipitating agents, respectively. These samples are labeled as Na−Al and K−Al. The X-ray diffraction patterns of the as-synthesized materials (Figure

**Table 1. Summary of Results upon Reconstruction of Calcined dawsonites in Different Media[a]**

| | | reconstruction | | | |
|---|---|---|---|---|---|
| precursor | synthesis pH[b] | medium | concentration (M) | pH[c] | product[d] |
| $NH_4$ dawsonite[e] | 8 | $(NH_4)_2CO_3$ | 2 | 10.5 | dawsonite |
| | 8 | $(NH_4)_2CO_3$ | 1 | 10 | dawsonite |
| | 8 | $(NH_4)_2CO_3$ | 0.5 | 9.5 | dawsonite |
| | 8 | $(NH_4)_2CO_3$ | 0.2 | 8.8 | amorphous |
| | 8 | $Na_2CO_3$ | 1 | 12 | Bayerite |
| | 8 | $Na_2CO_3$ | 0.1 | 10.9 | Bayerite |
| | 8 | $Na_2CO_3$ | 0.01 | 10.6 | Bayerite |
| | 8 | $K_2CO_3$ | 1 | 12 | Bayerite |
| | 8 | $K_2CO_3$ | 0.1 | 11.2 | Bayerite |
| | 8 | $K_2CO_3$ | 0.01 | 10.6 | Bayerite |
| Na dawsonite | 8 | $(NH_4)_2CO_3$ | 1 | 10 | dawsonite + Bayerite |
| | 8 | $Na_2CO_3$ | 1 | 12 | Bayerite |
| | 8 | $K_2CO_3$ | 1 | 12 | Bayerite |
| | 11 | $(NH_4)_2CO_3$ | 1 | 10 | dawsonite + Bayerite |
| K dawsonite | 8 | $(NH_4)_2CO_3$ | 1 | 10 | dawsonite |
| | 8 | $Na_2CO_3$ | 1 | 12 | Bayerite |
| | 8 | $K_2CO_3$ | 1 | 12 | Bayerite |

[a] The precursors were calcined at 723 K for 2 h. Other construction conditions: 323 K, 30 min, 350 rpm. [b] Constant pH during precipitation by the ILDP method. [c] Initial pH of the carbonate solution. [d] Phases detected by XRD. [e] This includes $NH_4-B_x-Al_{1+x}$, where B = Fe or Cr and $x = 0$ or 0.1.

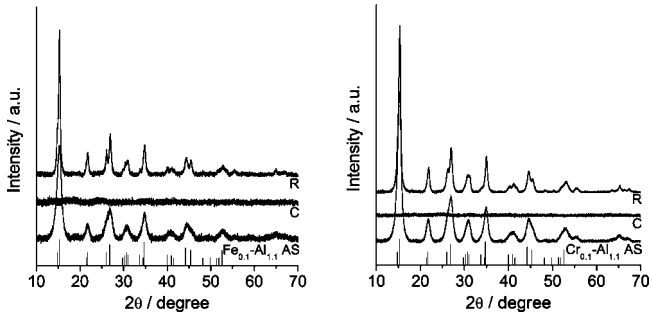


**Figure 4.** XRD patterns of the chromium and iron-substituted dawsonites and the products of calcination and reconstruction in 1 M $(NH_4)_2CO_3$ aqueous solution at 323 K for 30 min. Vertical lines belong to $NH_4AlCO_3(OH)_2$ (JCPDS 42-250).

5) showed dawsonite as the only crystalline phase, that is, $NaAlCO_3(OH)_2$ (JCPDS 45-1359) and $KAlCO_3(OH)_2$ (JCPDS 21-979). The calculated cell parameters for the sodium, ammonium, and potassium dawsonites correspond well with crystallographic data in the literature.[28,46,47] As visualized in Figure 1, the three forms of dawsonite have an orthorhombic lattice and are composed of the same $AlO_2(OH)_4$ chains of octahedra.[46] The different symmetries of $NH_4$ and K dawsonites (base-centered, space group *Cmcm*) and Na dawsonite (body-centered, space group *Imma*) render a larger *c* dimension in the former two materials.[30,46,47]

Thermal treatment of Na−AS and K−AS at 723 K leads to sodium aluminum oxide ($NaAlO_2$, JCPDS 2-985) and potassium aluminum oxide ($K_6Al_2O_6$, JCPDS 1-82-916), respectively. The occurrence of crystalline aluminates in Na and K dawsonites calcined above 900 K was previously reported.[48] In our case, the intensity of the $NaAlO_2$ reflections was considerably higher than that of the $K_6Al_2O_6$ reflections, suggesting a larger amount of the former crystalline phase. Therefore, the presence of amorphous alumina in the K dawsonite calcined at 723 K can be also expected. Additionally, the calcined Na−AS sample displayed distinctive reflections of sodium orthonitrate ($Na_3NO_4$, JCPDS 44-1051). $Na_3NO_4$ is likely derived from the reaction of residual sodium nitrate and sodium oxide formed upon thermal decomposition of Na dawsonite. However, no reflection of $NaNO_3$ was observed in the pattern of the as-synthesized Na dawsonite.

Treatment of the calcined materials in 1 M $(NH_4)_2CO_3$ aqueous solution (pH 10) at 323 K for 30 min originated the transformation into dawsonite by a dissolution−precipitation mechanism. Exceptionally, bayerite (α-$Al(OH)_3$, JPCPS 8-96) was observed as a secondary phase in the reconstructed sample derived from calcined Na dawsonite (see Figure 5). In great contrast, equivalent treatment of the calcined materials in sodium or potassium carbonate solutions induced no sign of dawsonite recovery. Instead, any of the calcined dawsonites fully transformed into bayerite (α-$Al(OH)_3$, JCPDS 8-96) on treatment in 1 M $Na_2CO_3$ (pH 12) or $K_2CO_3$ (pH 12) aqueous solutions for 30 min (Figure 5 and Table 1). A priori, bayerite crystallization can be associated with the excessively high pH of the 1 M sodium and potassium carbonate solutions. In good correspondence, thermodynamic studies by Bénézeth et al.[27] established that Na dawsonite is not stable at pH > 11.5, leading to bayerite as the predominant phase. In all our reconstruction treatments using 1 M ammonium carbonate (pH 10), the pH of the solution was monitored with time. As expected, the pH dropped from 10 to approximately 9.5 immediately after pouring the calcined samples in the carbonate solution followed by a slow decrease in the course of the treatment to values around 9.25−9.4 after 30 min (see example in Supporting Information).

The pH 10 of the 1 M ammonium carbonate solution is essential to convert the calcined samples into dawsonite, while pH ≥ 12 leads to bayerite (Table 1). As shown here and elsewhere,[8] pH ≥ 12 induces crystallization of aluminum hydroxides (bayerite and gibbsite), while pH = 6−7 (ammonium chloride and distilled water) leads to boehmite and diaspore. The relatively narrow pH window where the reconstruction occurs represents a limiting factor for potential

(46) Iga, T.; Kato, S. *J. Ceram. Soc. Jpn.* **1978**, *86*, 509.
(47) Fernandez-Carrasco, L.; Puertas, F.; Blanco-Varela, M. T.; Vázquez, T.; Rius, J. *Cem. Concr. Res.* **2005**, *35*, 641.
(48) Hernandez, M. J.; Ulibarri, M. A.; Cornejo, J.; Peña, M. J.; Serna, C. J. *Thermochim. Acta* **1985**, *94*, 257.

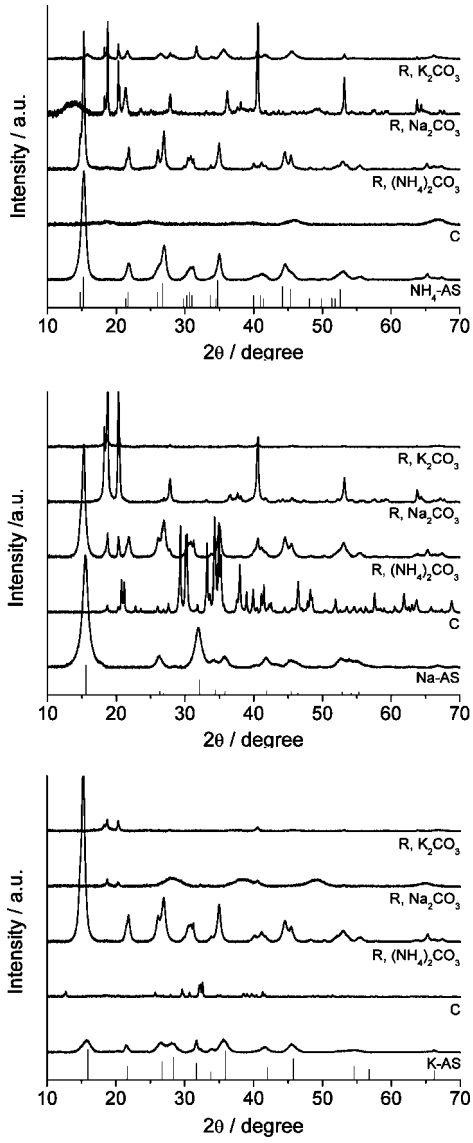


**Figure 5.** XRD patterns of the as-synthesized dawsonites in different forms ($NH_4$, K, Na−AS), the oxides resulting from calcination (C), and the products of treatment in 1 M $(NH_4)_2CO_3$, $K_2CO_3$, or $Na_2CO_3$ aqueous solutions at 323 K for 30 min (R).

application of Al-containing compounds in $CO_2$ mineralization. This is particularly relevant in the case of large pH fluctuations leading to dawsonite destabilization. Besides pH, the use of water as solvent is required. Treatment of alumina in 1 M $(NH_4)_2CO_3$ methanolic solution resulted in no transformation, although the attained value of the pH was 9.6. Alumina in aqueous solutions at pH > 6 first hydrates and then forms aluminate anions, $Al(OH)_4^-$. This does not occur with other protic solvents such as methanol. Subsequently, in analogy with Bénézeth et al.[27] for $NaAlCO_3(OH)_2$ synthesis, $NH_4$ dawsonite can precipitate according to the global reaction in eq 1. Tightly related to this, Zhang et al.[49] determined that the optimal conditions to synthesize dawsonite require moderately basic solutions (optimum at pH 10.3).

Originally, for systematic reasons, it was decided to compare samples derived from parent dawsonites synthesized by ILDP at the same pH (8), calcined at the same conditions (723 K for 2 h), and treated in solutions of carbonate salts with the same concentration (1 M) and conditions (temperature, time). As mentioned in the previous paragraph, fixing the concentration of the carbonate solution leads to treatments in the pH range of 10.5−12. Further insights into pH effects were obtained by varying the pH of the synthesis or comparing samples treated in different carbonate salts at the same initial pH. First of all, dawsonite recovery occurred independent of the synthesis pH of the parent $NH_4$, K, and Na dawsonites by precipitation (pH 8 and 11 were used), as long as 1 M $(NH_4)_2CO_3$ is used for reconstruction. Second, the concentration of the sodium and potassium carbonate solutions was lowered to approach the optimal value of 10 in 1 M $(NH_4)_2CO_3$. This was not strictly possible; the pH did not decrease below 10.6 (even if using very diluted solutions, 0.01 M) and bayerite was the only crystalline phase obtained (Table 1). The nearly identical pH between a 2 M $(NH_4)_2CO_3$ solution (10.5, where reconstruction occurs) and a 0.01 M $Na_2CO_3$ solution (10.6, where bayerite is obtained) suggests the specificity of the ammonium cation in inducing reconstruction. However, it should be mentioned that the concentration of carbonate ions (required to transform $Al_2O_3$ into $NH_4AlCO_3(OH)_2$) is much higher in 2 M $(NH_4)_2CO_3$ than in a 0.01 M $Na_2CO_3$.

The formation of bayerite as a residual phase on treatment of calcined Na dawsonites in $(NH_4)_2CO_3$ can be tentatively related to the local increase in alkalinity by dissolution of sodium orthonitrate, favoring aluminum reprecipitation as crystalline $Al(OH)_3$. The latter is supported by the absence of both $Na_3NO_4$ and $NaAlO_2$ in the pattern of the reconstructed sample. In fact, as shown in Supporting Information, the evolution of pH versus time in the solution of calcined Na dawsonite decreases slower than that of calcined $NH_4$ dawsonite and K dawsonite. As a result, despite the significant changes in the first 5 min, the final pH of $NH_4$ and K coincided while that of Na was higher. Surprisingly, the unique ability of $(NH_4)_2CO_3$ to reconstruct dawsonite is not exclusively applicable to amorphous alumina (derived from $NH_4$ dawsonite) but additionally to alkaline aluminas or aluminates (derived from Na and K dawsonites at 723 K). Broadening the range of Al-containing compounds able to form dawsonite requires further investigation.

**Mechanism of Alumina Carbonation.** The evolution of alumina to dawsonite was followed by thermogravimetric analysis and infrared spectroscopy to gain additional mechanistic insights into the reconstruction process. Herein, we elaborate on the treatment of the calcined $NH_4$ dawsonite under standard conditions (1 M $(NH_4)_2CO_3$ aqueous solution, $(NH_4)_2CO_3/Al_2O_3 = 25$, and 323 K). The investigation concentrates on the first 30 min, that is, the period where most significant changes in X-ray diffraction occurred (see Figure 2).

Thermogravimetric analyses of the solid samples treated at different times (after filtration and drying) made it possible to monitor the reconstruction process and to estimate the degree of dawsonite recovery with time. As shown in Figure 6 (left), the as-synthesized sample (AS) presents a characteristic one-step weight loss of approximately 50% centered

(49) Zhang, X,.; Wen, Z.; Gu, Z.; Xu, X.; Lin, Z. *J. Solid State Chem.* **2004**, *177*, 849.

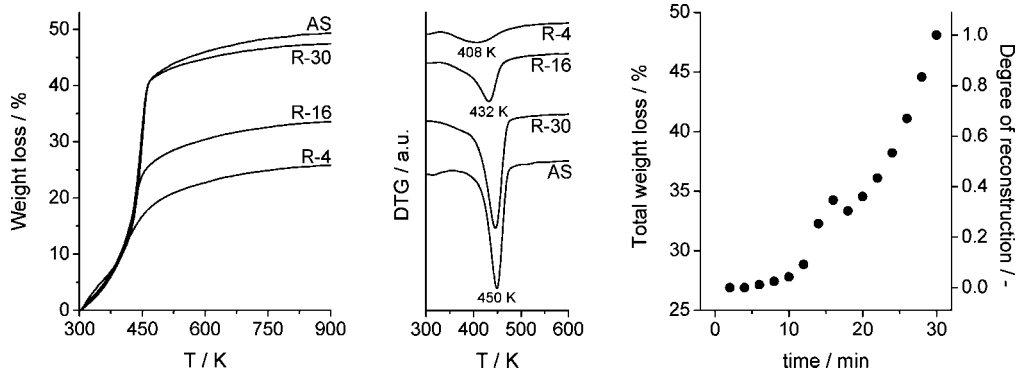


**Figure 6.** Thermogravimetric profiles (left) and derivative of the weight loss (center) of selected samples upon decomposition in air at 5 K $min^{-1}$. The right figure plots the total weight loss of the samples and calculated degree of reconstruction versus the reconstruction time.

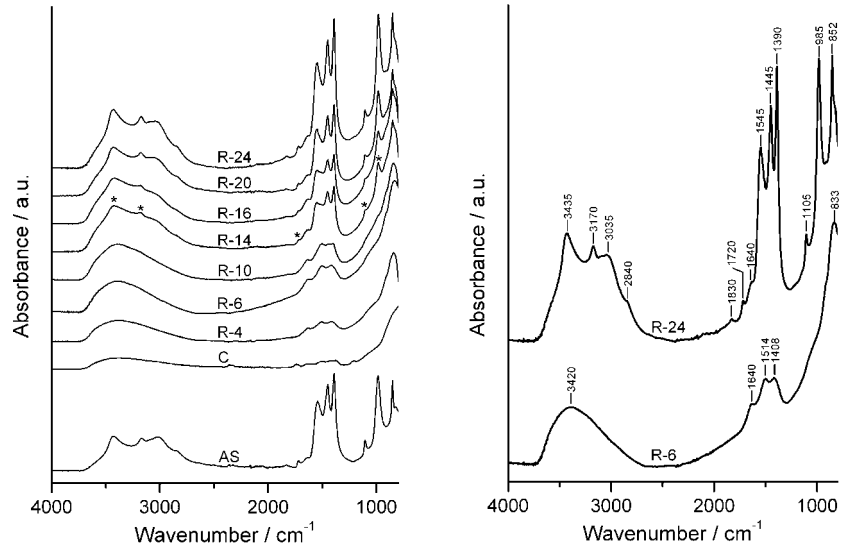


**Figure 7.** FTIR spectra during reconstruction of AACH-derived alumina in 1 M $(NH_4)_2CO_3$ at 323 K and different times. The spectra of the as-synthesized sample and calcined samples are shown for reference.

at 450 K, which has been assigned to the decomposition of ammonium aluminum carbonate hydroxide.[8,32] The total weight loss of the treated samples increases upon increasing the duration of the treatment (e.g., 26% in R-4, 35% in R-16, and 47% in R-30). This information is more complete in Figure 6 (right), where the total weight loss of the treated solids every 2 min in the period 0−30 min is plotted. The weight loss in the first 10 min of the treatment was practically constant (ca. 26%) and steeply increased on longer treatments, reaching 47% after 30 min.

The weight loss of the samples at $t < 10$ min is assigned to the decomposition of an intermediate phase in the transition from $Al_2O_3$ and $NH_4AlCO_3(OH)_2$, which is amorphous according to X-ray diffraction results. This compound was identified and characterized by FTIR. Figure 7 shows the infrared spectra of the AS and C samples and the solids at selected reconstruction times. The AS sample shows characteristic bands of the hydroxyl, ammonium, and carbonate groups in dawsonite,[8,30] which practically disappear in the calcined sample. In the first stages of the treatment in $(NH_4)_2CO_3$ ($t < 10$ min), the material progressively develops bands in the hydroxyl and carbonate regions. As illustrated more specifically in Figure 7, the sample R-6 (0% reconstruction) shows a broad adsorption band at 3420 $cm^{-1}$ attributed to OH stretching in $Al(OH)_3$, a band at 1640 $cm^{-1}$ corresponding to OH bending, and bands corresponding to carbonate groups ($\nu_3$ at 1514 $cm^{-1}$ and 1408 $cm^{-1}$ and $\nu_2$ at 835 $cm^{-1}$). These fingerprints are unequivocal evidence for the presence of carbonate-containing aluminum hydroxide as intermediate phase in early stages of the reconstruction process corresponding to the amorphous phase anticipated by X-ray diffraction and thermogravimetry. Our assignment is based on infrared characterization communicated by several authors,[33,50] who explicitly reported the amorphous nature of this compound.

The steep weight loss increase experienced by the samples at $t > 10$ min is attributed to the progressive formation of dawsonite. The time scale agrees very well with the appearance of the dawsonite phase in XRD analyses (Figure 2). The thermogravimetric profile and total weight loss of R-30 practically matched those of AS, indicating that the dawsonite reconstruction was completed after 30 min. Considering the weight loss of the R-2 and R-30 samples as 0% and 100% reconstruction, the degree of dawsonite recovery versus the treatment time can be determined. This quantification is illustrated in Figure 6,

(50) Scholtz, E. C.; Fedlkamp, J. R.; White, J. L.; Hem, S. L. *J. Pharm. Sci.* **1984**, *73*, 967.

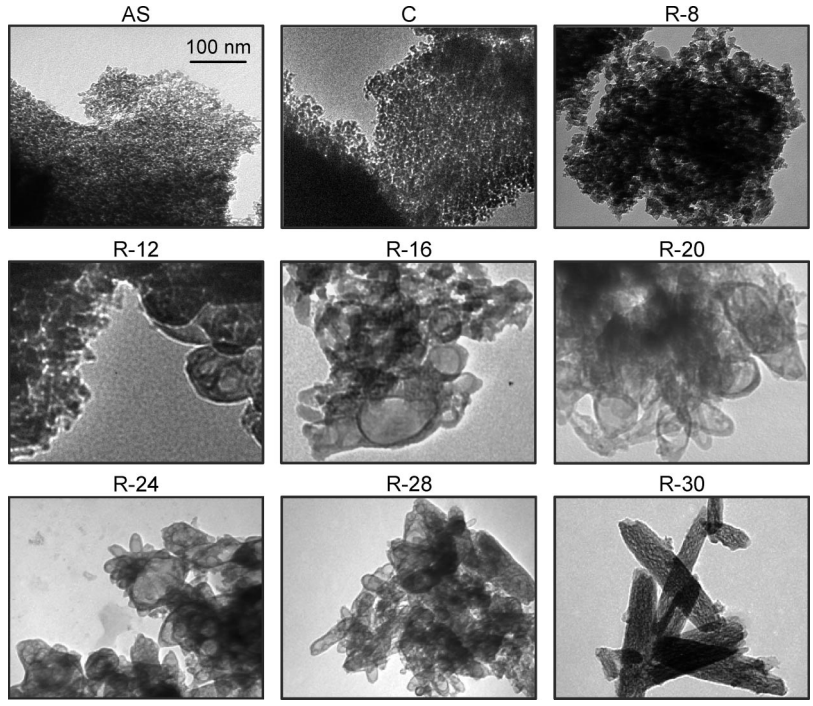


**Figure 8.** TEM micrographs of the as-synthesized, calcined, and treated samples at different times. The scale bar applies to all the samples. The starting dawsonite was in the ammonium form, and the oxide reconstruction was conducted in 1 M $(NH_4)_2CO_3$ aqueous solution at 323 K.

right. The derivative of the weight loss (Figure 6, center) provides additional information on the evolution of the phases in the solids along the treatment. As expected, the fully reconstructed R-30 and the as-synthesized samples show the same transition temperature, that is, 450 K. The transition temperature is shifted to lower temperature at shorter times. For example, R-4 (0% reconstruction) displays a transition temperature of 408 K, indicating the lower stability of the intermediate amorphous phase compared to dawsonite. As expected, the transition temperature of R-16 (35% reconstruction, 432 K) is intermediate between that of R-4 and R-30.

The time at which dawsonite is first identified in the infrared spectra is in excellent agreement with XRD and TGA (Figure 6). On the basis of assignments made elsewhere,[8,28] the marked changes in the spectrum of R-14 (see asterisks) is a consequence of the incipient crystallization of dawsonite:

(i) Characteristic $NH_4^+$ vibrations, which were absent in the intermediate phase, appear at 3170, 3005, and 2840 $cm^{-1}$ ($\nu_{NH}$) and 1830 and 1720 $cm^{-1}$ ($\delta_{NH}$).

(ii) The broad OH stretching vibration at 3420 $cm^{-1}$ in $Al(OH)_3$ shifts to the characteristic absorption at 3435 $cm^{-1}$ in $NH_4AlCO_3(OH)_2$.

(iii) Characteristic vibrations of $CO_3^{2-}$ groups in $NH_4AlCO_3(OH)_2$ are distinguished, that is, $\nu_3$ at 1545, 1445, and 1387 $cm^{-1}$, $\nu_1$ at 1105 $cm^{-1}$, $\nu_2$ at 852 $cm^{-1}$. This implies a drastic reorganization of the carbonates upon crystallization of the dawsonite phase. The vibration at 1514 $cm^{-1}$ in R-6 shifts to 1545 $cm^{-1}$ in R-24 and the vibration at 1408 $cm^{-1}$ splits into two carbonate bands at 1445 $cm^{-1}$ and 1390 $cm^{-1}$ as a consequence of a decreased carbonate symmetry, leading to the appearance of the 1105 $cm^{-1}$ band in the reconstructed sample.

(iv) A sharp vibration band at 985 $cm^{-1}$, assigned to Al−OH deformation in dawsonite, is evidenced.

As expected, the above assigned vibrations sharpen as the reconstruction of dawsonite proceeds.

**Morphology and Textural Changes during Reconstruction.** Transmission electron microscopy and $N_2$ adsorption measurements were used to monitor the morphological and textural transformations of the as-synthesized material upon calcination and subsequent reconstruction. The TEM micrograph of the AS sample shows the presence of aggregated relatively uniform spherical-like aggregates (<10 nm), which are mostly preserved after calcination at 723 K (Figure 8). It can be anticipated that clusters of small particles will induce a high degree of interparticle porosity in both samples. This is indeed confirmed by $N_2$ porosity showing a combined type I and IV isotherm, following IUPAC guidelines (Figure 9).[51] The presence of mesopores is responsible for the type IV behavior while the enhanced uptake at lower relative pressures (corresponding to type I) denotes the presence of micropores. Application of the *t*-plot confirms the combined micro- and mesoporous character, a substantial micropore volume of 0.10 $cm^3\ g^{-1}$ (Table 2), and a contribution of mesoporosity amounting to 555 $m^2\ g^{-1}$. The isotherm of the calcined alumina sample reflects similar porous characteristics in the mesopore regime as the AS sample, though lacking the distinct uptake at low relative pressure. The latter observation strongly suggests the absence of microporosity in the calcined sample, which is supported by the *t*-plot results in Table 2 evidencing a purely mesoporous material. These changes in porosity induce a decrease in BET surface

(51) Sing, K. S. W.; Everett, D. H.; Haul, R. A. W.; Moscou, L.; Pierotti, R. A.; Rouquerol, J.; Siemieniewska, T. *Pure Appl. Chem.* **1985**, *57*, 603.

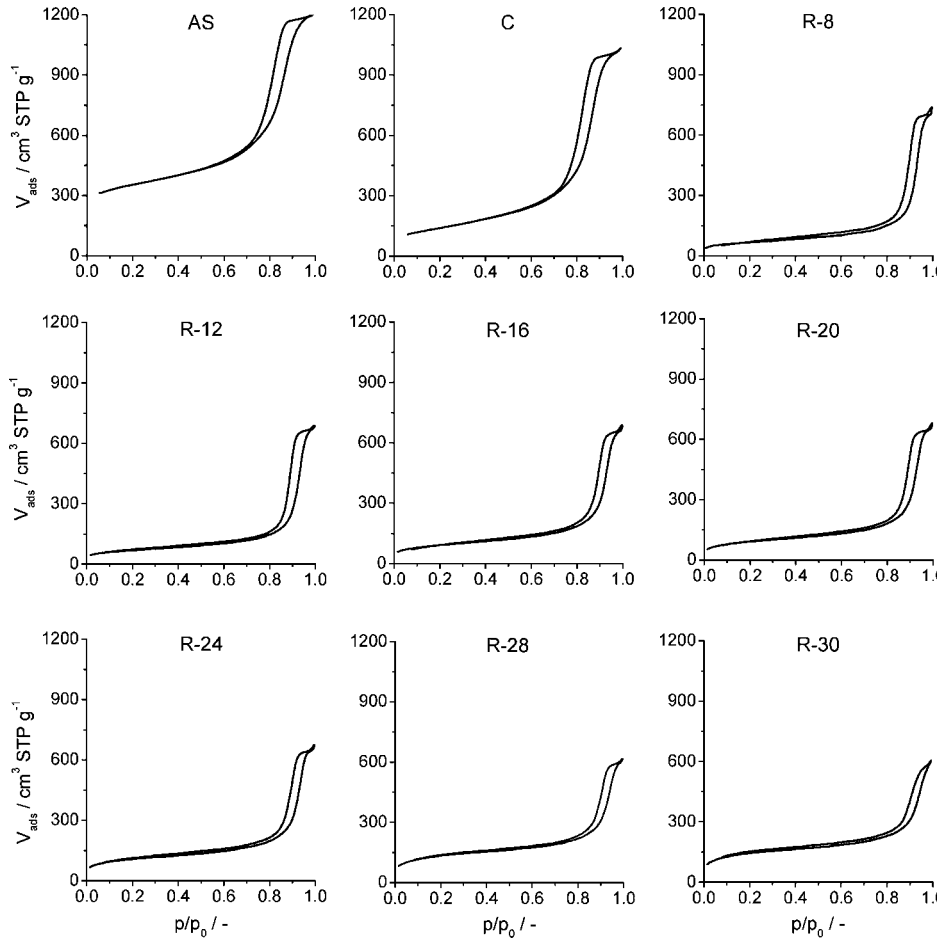


**Figure 9.** Nitrogen isotherms at 77 K of the as-synthesized, calcined, and reconstructed samples.

**Table 2. Textural Characterization of Selected Samples**

| sample code[a] | $V_{pore}$ (cm$^3$ g$^{-1}$) | $V_{micro}$[b] (cm$^3$ g$^{-1}$) | $S_{meso}$[b] (m$^2$ g$^{-1}$) | $S_{BET}$[c] (m$^2$ g$^{-1}$) |
|---|---|---|---|---|
| AS | 1.60 | 0.10 | 555 | 773 |
| C | 1.40 | 0.00 | 500 | 500 |
| R-8 | 1.10 | 0.02 | 189 | 236 |
| R-12 | 1.05 | 0.03 | 176 | 240 |
| R-16 | 1.03 | 0.05 | 218 | 316 |
| R-20 | 1.02 | 0.05 | 210 | 319 |
| R-24 | 1.02 | 0.07 | 210 | 371 |
| R-28 | 0.94 | 0.12 | 198 | 462 |
| R-30 | 0.90 | 0.14 | 197 | 497 |

[a] AS: as-synthesized $NH_4$ dawsonite sample. C: calcined sample. R-*x*: reconstructed samples. The number *x* indicates the reconstruction time in minutes at 323 K. [b] *t*-plot method. [c] BET method.

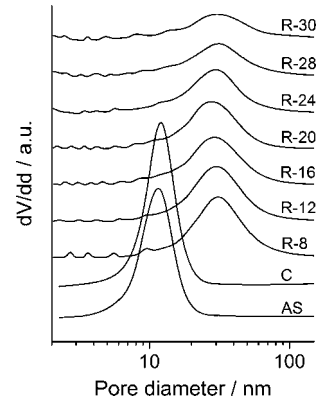


**Figure 10.** BJH desorption pore size distribution of the samples derived from the $N_2$ isotherms.

area from 773 m$^2$ g$^{-1}$ in AS to 500 m$^2$ g$^{-1}$ in C. The BJH pore size distributions conclude a similar narrow distribution of mesopores centered at 10 nm (Figure 10).

Treatment of alumina in $(NH_4)_2CO_3$ solution for 8 min leads to moderate morphological changes as depicted in the TEM micrographs and rendered a material with larger, irregular, and agglomerated particles. As a consequence, the adsorption isotherm displays a hysteresis loop at higher relative pressures with a lower $N_2$ uptake, pointing to the presence of larger mesopores. The latter is clearly substantiated by the shift in the maximum of the pore size distribution from 10 to 30 nm. Only after longer treatment times marked changes in the morphology occur (see R-12). New architectures of bigger spherical-like particles with a darker outer rim and a lighter layer core appear. The latter observation suggests the presence of a denser phase in the edges likely corresponding to the dawsonite phase that starts to develop. With increasing reconstruction time, also the micropore volume progressively increases. This can tentatively be attributed to the formation of the dawsonite phase that typically is microporous.[8] This in turn provokes an enhanced total BET surface area, as the mesoporosity is kept fairly constant.

At longer reconstruction times, the outer rim becomes thicker, enabling the hypothesis that $NH_4^+$ and $CO_3^{2-}$ species gradually diffuse from the outside to the center of the particle, driving the progressive precipitation of dawsonite and resulting in a further increase in microporosity. In excellent

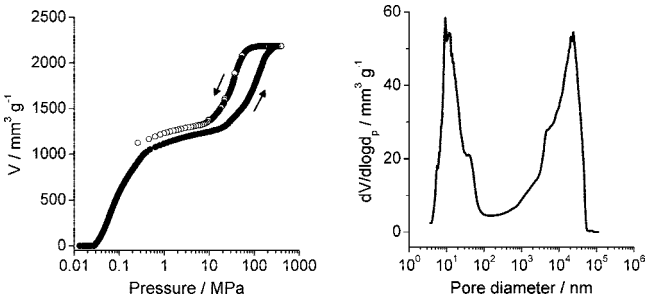


**Figure 11.** Hg intrusion (solid symbols) and extrusion (open symbols) curves of R-20 (left) and derived pore size distribution using the Washburn equation (right).

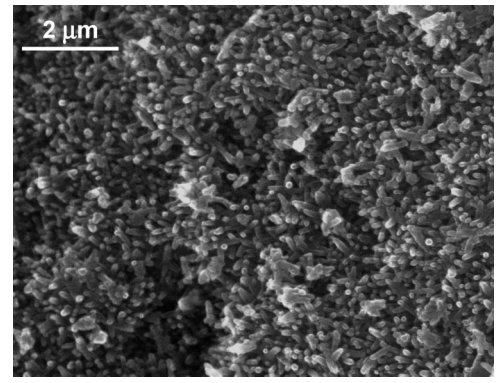


**Figure 12.** Scanning transmission micrograph of R-30.

agreement, XRD reflections and IR absorption bands of the ongoing dawsonite formation appear in the same time range correlating with the changes in morphology. The latter observations suggest a phase transition from the amorphous carbonate-containing aluminum hydroxide phase to dawsonite. As the reconstruction process proceeds (R-20 to R-24), the contrast in the zoned particles becomes more uniform suggesting an increase of the material density as dawsonite recrystallizes. As the TEM micrographs tentatively suggest the presence of hollow porous particles, mercury intrusion porosimetry was applied to assess the accessibility of the porosity as determined by $N_2$ adsorption. The intrusion and extrusion curves acquired over sample R-20 show a two-step behavior (Figure 11). The step at low pressure is attributed to the voids between the aggregates whereas the second transition at higher pressure is the result of interparticle porosity. The interparticle volume of approximately 0.95 $cm^3\ g^{-1}$ associated with the latter step is in excellent agreement with the porous properties derived from $N_2$ adsorption. The full reversibility of the intrusion and extrusion curve coupled to the good correlation between both pore size distributions further evidence that the porosity is readily accessible and not encapsulated within the apparent partially hollow particles. From R-24 to R-30, the morphology evolves toward the more thermodynamically favored acicular crystals specific to the dawsonite mineral.[52] Related to this, Ma et al.[53] observed that pH > 8 induced formation of acicular to stick fibers rather than the disordered hairy particles obtained at pH < 7. Scanning electron microscopy also evidences the acicular geometry of the reformed dawsonite crystals (Figure 12). Similar morphological and textural transformations leading to acicular configurations were also observed at other reconstruction conditions.

## Conclusions

Aluminas derived from thermal decomposition of dawsonite-type compounds exhibit structural memory; that is, the original mineral structure in ammonium form ($NH_4AlCO_3(OH)_2$) is recovered by treatment in aqueous solutions of ammonium carbonate under mild conditions at pH ~ 10. Alumina carbonation to dawsonite is specific to $(NH_4)_2CO_3$, and the memory property applies to dawsonite compounds with different compensating cations ($NH_4^+$, $K^+$, $Na^+$) and also with substitution by transition metals ($Fe^{3+}$, $Cr^{3+}$) in $Al^{3+}$ positions of the framework. In great contrast, treatment of calcined dawsonites in other carbonate-containing solutions salts such as $K_2CO_3$ and $Na_2CO_3$ leads to bayerite. Similarly to layered double hydroxides with hydrotalcite structure, the term memory is used since we start from the dawsonite structure, decompose it by thermal treatment, and recover it upon specific treatment and conditions. Accordingly, calcined dawsonite "remembers" the way back to dawsonite, and this transformation is thermodynamic and kinetically favored. The kinetics and mechanism of the reconstruction process have been successfully studied. The alumina-to dawsonite transition is relatively fast (10−30 min depending on the temperature) and follows a dissolution−precipitation mechanism. By this, alumina forms an amorphous carbonate-containing aluminum hydroxide phase followed by dawsonite recrystallization. The original and reconstructed dawsonites present striking morphological and porosity differences. Nanoparticles in the as-made and calcined materials transformed through complex intermediate morphologies into well-crystallized acicular nanoneedles with newly developed microporosity in the reconstructed material. Our results can be of significance to improve current applications of dawsonites associated with the modified properties induced by the memory effect. Besides, this work opens a route for $CO_2$ mineralization using Al-containing compounds through dawsonite formation.

**Acknowledgment.** This research was supported by the Spanish MEC (Project No. CTQ2006-01562/PPQ, Consolider-Ingenio 2010 Grant CSD2006−003) and the ICIQ Foundation. G.S. is the recipient of a Ph.D. fellowship from the FPU Program (AP2005-5147), and S.A. is a Torres Quevedo fellow (PTQ05-01-00980). J.P.-R. is indebted to the Journal Grants Scheme of the Royal Society of Chemistry.

**Supporting Information Available:** Plot of evolution of pH with time during reconstruction of calcined $NH_4$, Na, and K dawsonites (PDF). This material is available free of charge via the Internet at http://pubs.acs.org.

CM800359T

(52) Anthony, J. W.; Bideaux, R. A.; Bladh, K. W.; Nichols, M. C. *Handbook of Mineralogy*; Mineral Data Publishing: Tucson, AZ, 2007, Vol. V, p 176.
(53) Ma, C.-C.; Zhou, X.-X.; Xu, X.; Zhu, T. *Mater. Chem. Phys.* **2001**, *72*, 374.